

Bragg reflection from equidistant planes of vortex sheets in rotating $^3\text{He-A}$

Ü. Parts, J. H. Koivuniemi, M. Krusius, V. M. H. Ruutu,
and E. V. Thuneberg

Low Temperature Laboratory, Helsinki University of Technology, 02150 Espoo, Finland

G. E. Volovik

*Low Temperature Laboratory, Helsinki University of Technology, 02150 Espoo, Finland;
Landau Institute for Theoretical Physics, RAS, 117334 Moscow, Russia*

(Submitted 12 May 1994)

Pis'ma Zh. Eksp. Teor. Fiz. **59**, No. 12, 816–820 (25 June 1994)

Recently a new state of rotating superfluid $^3\text{He-A}$, which consists of equidistant planes of vortex sheets, was discovered. Its cw NMR absorption spectrum includes a small satellite peak which has the largest relative frequency shift ever observed in $^3\text{He-A}$. This peak is attributed to the excitation of a stationary spin wave mode which is localized in the gaps between the vortex sheets. This mode corresponds to the first Bragg reflection from a one-dimensional periodic potential. The frequency shift provides a measurement of the distance between vortex sheets. This distance agrees with the prediction of Landau and Lifshitz in 1955.

Many different structures of quantized vorticity have been found to exist in ^3He superfluids when they are rotated in a cylindrical container at an angular velocity Ω . A new state of vorticity has recently been identified in NMR measurements on the anisotropic $^3\text{He-A}$ phase.¹ This state was found to consist of vortex sheets. The sheets are parallel to the rotation axis Ω and are separated by layers of vortex-free superflow. Similar to vortex lines, the sheets allow the solid-body-like rotation of the superfluid on a macroscopic scale. The distance b between the sheets, which is determined by the competition of the kinetic energy of the counterflow, $\frac{1}{2} \rho_s (\mathbf{v}_s - \mathbf{v}_n)^2$, and the surface tension σ of the sheets, was found by Landau and Lifshitz²

$$b = \left(\frac{3\sigma}{\rho_s \Omega^2} \right)^{1/3} \quad (1)$$

in an attempt to understand the rotating state of superfluid ^4He .

The vortex soliton which forms the sheet in $^3\text{He-A}$ is a combination of a two-dimensional domain wall (called a soliton) and one-dimensional vortices. The wall is between domains having parallel ($\hat{\mathbf{l}} = \hat{\mathbf{d}}$) and antiparallel ($\hat{\mathbf{l}} = -\hat{\mathbf{d}}$) orientations of $\hat{\mathbf{l}}$ and $\hat{\mathbf{d}}$. Here $\hat{\mathbf{l}}$ and $\hat{\mathbf{d}}$ are the orbital and magnetic anisotropy axes, respectively. The vorticity accumulated in the soliton is nonsingular, i.e., it arises from an inhomogeneous $\hat{\mathbf{l}}$ texture which is periodic along the vortex sheet in the direction perpendicular to Ω . Estimating the surface tension under our experimental conditions, we can calculate from Eq. (1) that $b \approx 360 \Omega^{-2/3} \mu\text{m}$ (with Ω in rad/s).¹

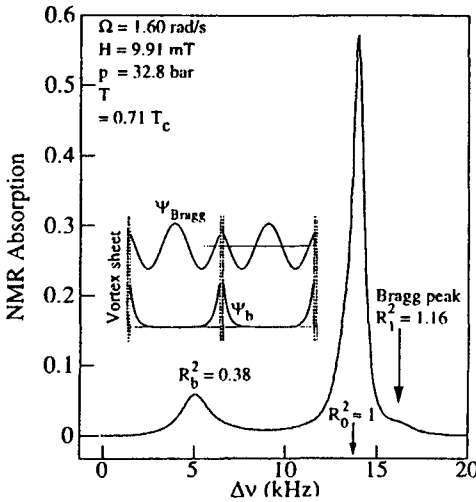


FIG. 1. The cw NMR absorption of the vortex-sheet state as a function of the frequency shift, $\Delta\nu = \nu - \nu_0$, from the Larmor frequency ν_0 . The peak with the lowest frequency R_b arises from a bound state which is localized on the vortex sheet, while the other two peaks come from the continuum states. The largest peak at R_0 is approximately at the same frequency as the bulk liquid absorption in the nonrotating equilibrium state. The Bragg reflections from successive vortex sheets give rise to the small peak at R_1 .

The purpose of this letter is to show that b can be directly extracted from the measurement of the frequencies of three peaks in the NMR absorption spectrum. Figure 1 shows the cw NMR absorption as a function of excitation frequency in the vortex-sheet state. The frequency of an absorption maximum is conventionally expressed as $\omega^2 = \omega_0^2 + R_{\perp}^2 \omega_{\parallel}^2$, where $\omega_0 = \gamma H$ is the Larmor frequency, and the ω_{\parallel} is the temperature- and pressure-dependent longitudinal resonance frequency of the A phase. The dominant peak at $R_{\perp} = R_0 \approx 1$ originates from the dipole-locked ($\hat{\mathbf{i}} = \pm \hat{\mathbf{d}}$) bulk liquid. The low-frequency satellite peak at $R_{\perp}^2 = R_b^2 = 0.38$ is the signature of the vortex soliton.¹ It arises from a spin-wave mode which is localized at the sheet because of the attractive potential caused by dipole unlocking ($\hat{\mathbf{i}} \neq \pm \hat{\mathbf{d}}$).

The crucial new feature in Fig. 1 is the smaller satellite at higher frequency, $R_{\perp}^2 = R_1^2 = 1.16$. It is to date the only clear observation of an absorption maximum in the continuum region with $R_{\perp} > 1$. It can be understood as a Bragg reflection from a one-dimensional potential, which is created by the periodic sequence of vortex sheets. The Bragg reflection of spin waves from a lattice of vortex lines was originally suggested by Fomin and Kamenskii.³ We conclude that the reflections from the vortex sheets produce larger intensities than from the two-dimensional vortex lattice, because in the latter case no Bragg peak has yet been observed.

The frequency R_b of the low-frequency satellite was found to be independent of Ω . In contrast, the new peak has a frequency R_1 , which increases with Ω . In Fig. 2 the measured R_1^2 is plotted as a function of Ω . The result fits the dependence $R_1^2 - 1 = 0.090 \Omega^{4/3}$. The intensities of the two satellites display opposite Ω dependences: while the intensity of the low-frequency peak increases proportionally to the total area of the vortex soliton, $\propto b^{-1} \propto \Omega^{2/3}$, the intensity of the high-frequency maximum decreases with Ω , as shown in Fig. 3. All measurements were carried out in a magnetic field $\mathbf{H} \parallel \boldsymbol{\Omega} \parallel \hat{\mathbf{z}}$, and the data analysis is for the temperature $T = 0.71 T_c$ and pressure $p = 32.8$ bar. The state with vortex sheets was created as described in Ref. 1.

The experimental results can be understood semiquantitatively as follows. Locally

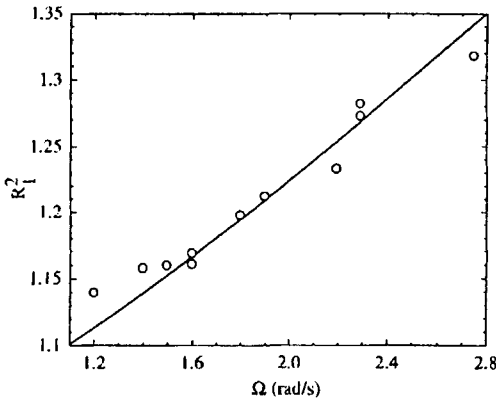


FIG. 2. Measured Ω dependence of the frequency shift R_1^2 of the Bragg peak. The solid line is a fit to the data with $R_1^2 = 1 + 0.090 \Omega^{4/3}$, which obeys the Ω dependence of Eq. (6).

the sheets can be considered as planar and we fix $\hat{\mathbf{x}}$ as their normal. In our case $\mathbf{H} \parallel \boldsymbol{\Omega} \parallel \hat{\mathbf{z}}$ the equilibrium $\hat{\mathbf{d}}$ is approximately constant: $\hat{\mathbf{d}}_0 \approx \hat{\mathbf{y}}$. The NMR excitation causes the spin magnetization to precess and forces small oscillations of $\hat{\mathbf{d}}$ parallel to \mathbf{H} : $\hat{\mathbf{d}} = \hat{\mathbf{d}}_0 + \Psi \hat{\mathbf{z}} \cos(\omega t)$. The eigenmodes obey the Schrödinger equation^{4,5}

$$-\xi_{D\perp}^2 \frac{d^2 \Psi}{dx^2} + V\Psi = (R_{\perp}^2 - 1)\Psi, \quad (2)$$

where the dipole length $\xi_{D\perp} = \sqrt{K_6}$, $\xi_D \approx 9.8 \mu\text{m}$ (Ref. 6) and the potential $V = -(2\hat{l}_z^2 + \hat{l}_x^2)$. There is a potential well at each sheet, whose depth is on the order of unity and whose range is on the order of the soliton thickness, $s \sim \xi_{D\perp}$. The thickness s is small compared to the distance b between the sheets, $s \ll b$.

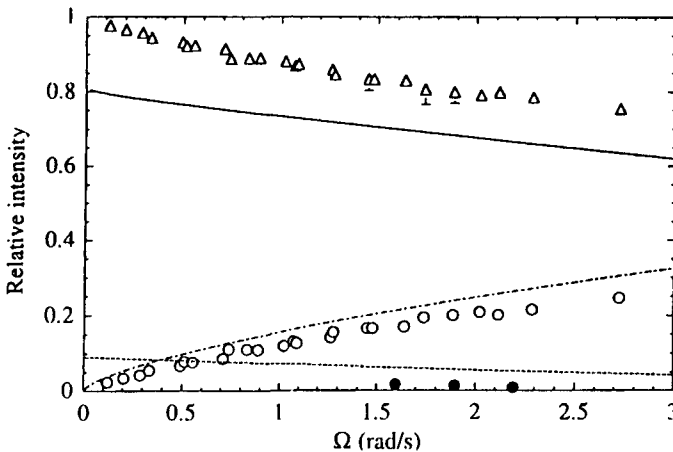


FIG. 3. Integrated NMR absorptions of the three-peaks shown in Fig. 1, normalized to the total absorption of the NMR signal, and plotted as a function of Ω . Δ —Bulk liquid peak at R_0 ; \circ —low-frequency satellite at R_0 ; \bullet —high-frequency satellite at R_1 . The lines represent Eq. (7) with $a = 1.6 \xi_{D\perp}$ and $b(\Omega$ from Fig. 4.

In general, the potential V is known only numerically. The simplest approximation, which we will discuss first, is to assume a delta-function form:

$$V(x) = -a \sum_j \delta(x - jb). \quad (3)$$

With this model the bound state is

$$R_b^2 - 1 = -\frac{a^2}{4\xi_{D\perp}^2}. \quad (4)$$

Since experimentally $R_b^2 = 0.38$ (Fig. 1), we can determine the potential parameter $a = 1.6\xi_{D\perp}$.

Only those eigenstates with nonzero $\int dx \Psi$ couple to the uniform NMR excitation. In the continuum they are the standing waves of the form $\Psi_n(x) \propto \cos(q_n[x - (j + \frac{1}{2})b])$ in the interval $jb < x < (j+1)b$. Here q_n is the n th positive root of the equation

$$u_n \tan \frac{u_n}{2} = -\gamma, \quad u_n = q_n b \quad \text{and} \quad \gamma = \frac{ab}{2\xi_{D\perp}^2}. \quad (5)$$

The eigenvalues are $R_n^2 - 1 = \xi_{D\perp}^2 q_n^2$. We see that the main peak, which corresponds to the mode $n=0$, is slightly shifted to a higher frequency from its position $R_0=1$ in the nonrotating liquid. This is also experimentally the case. For the relative shift of the first Bragg peak (mode $n=1$) we obtain

$$R_1^2 - R_0^2 = (u_1^2 - u_0^2) \frac{\xi_{D\perp}^2}{b^2}. \quad (6)$$

Taking R_1^2 from Fig. 2, we solve Eqs. (5) and (6) self-consistently. In the limit $\Omega \rightarrow 0$, where b and γ diverge, these equations are solved by $b = \pi \xi_{D\perp} \sqrt{8/(R_1^2 - R_0^2)} \approx 290 \Omega^{-2/3} \mu\text{m}$. The self-consistently calculated $b(\Omega)$ is shown in Fig. 4. It can be fitted as $b \approx 320 \Omega^{-2/3} \mu\text{m}$. This value is close to the value $b \approx 360 \Omega^{-2/3} \mu\text{m}$, which was originally estimated from Eq. (1) in Ref. 1.

The relative intensities of the absorption peaks can be calculated from the formula $I/I_{\text{tot}} = (\int dx \Psi)^2 / (b \int dx \Psi^2)$. For the three absorption peaks we obtain

$$\frac{I_b}{I_{\text{tot}}} = 8 \frac{\xi_{D\perp}^2}{ab}, \quad \frac{I_0}{I_{\text{tot}}} = \frac{8}{u_0^2} \frac{\sin^2 \frac{u_0}{2}}{1 + \frac{\sin u_0}{u_0}}, \quad \frac{I_1}{I_{\text{tot}}} = \frac{8}{u_1^2} \frac{\sin^2 \frac{u_1}{2}}{1 + \frac{\sin u_1}{u_1}}. \quad (7)$$

These expressions are compared in Fig. 3 to the measured intensities as a function of Ω . The uncertainty in the measured intensity is smaller than 4% for the two large peaks, while for the high frequency peak it is on the order of 100%, because of the strong overlap with the main peak. The theoretical and measured intensities of the bound-state peak are close to each other, despite the crudity of the model (3). For the Bragg peak the

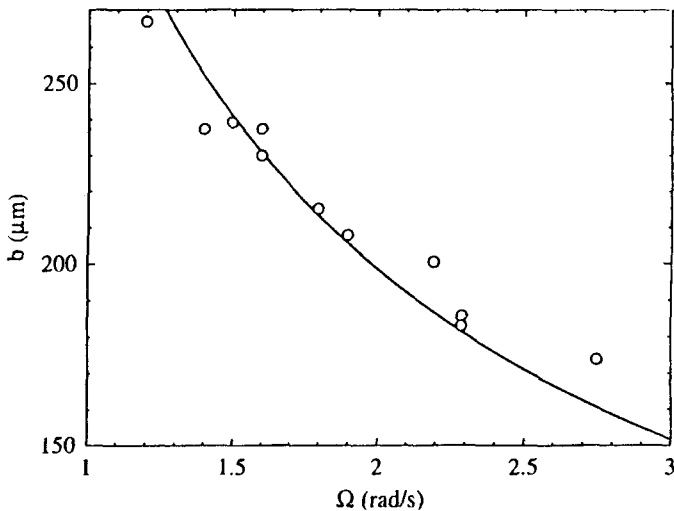


FIG. 4. Vortex-sheet separation $b(\Omega)$. The data for the frequency shifts in Figs. 1 and 2 were converted to $b(\Omega)$ using Eqs. (4)–(6). The line is a fit to the $b(\Omega)$ data points with the $\Omega^{-2/3}$ dependence from Eq. (1), giving $b = 320 \Omega^{-2/3} \mu\text{m}$ (with Ω in rad/s).

calculated intensity is several times higher than the measured. Its monotonic decrease from the $\Omega \rightarrow 0$ limiting value, $8/(3\pi)^2$, nevertheless reproduces the experimental behavior.

The delta-function approximation (3) is valid in the limit in which the extension of the wave function essentially exceeds the thickness s of a vortex sheet. This is satisfied for the lowest Bragg states whose wavelength $\lambda \sim b \gg s$. For the bound states this value is marginal, because the decay length of the wave function $2\xi_{D\perp}^2/a$ is of the same order of magnitude as the range of the true potential. A more correct approach is to consider the potential in Eq. (3) only for the modes in the continuum region, while a should be extracted from the integration $a = -\int dx V$ over the exact potential in the vortex soliton, instead of using Eq. (4). One way of accomplishing this goal is to take the limit of low velocity¹ $\Omega \rightarrow 0$. We will consider this limit for comparison, although the data of the Bragg peak exist only at relatively high velocities, $\Omega > 1$ rad/s. The vortex sheet consists of alternating twist and bend textures of $\hat{\mathbf{l}}$. At small Ω the vortices in the sheet are far apart and the twist sections dominate. For the twist section we obtain $a = 4\xi_D \sqrt{K_t} \approx 2.4\xi_{D\perp}$ in the notation of Ref. 6. This estimate provides an upper limit for a to be achieved at the slowest rotation, because the potential is deepest at the twist section. Fitting this estimate to the data gives $b \approx 280 \Omega^{-2/3} \mu\text{m}$. The intensity of the bound state in this model is

$$\frac{I_b}{I_{\text{tot}}} = \frac{\xi_D \sqrt{\pi K_t}}{b} \frac{\Gamma(n+1/2)\Gamma^2(n/2)}{\Gamma(n)\Gamma^2[(n+1)/2]}, \quad (8)$$

where $n = (\sqrt{1 + 8K_t/K_6} - 1)/2$. This result is a factor of 1.2 larger than the result of the delta-function model plotted in Fig. 3.

Another omission above is that the potential is not constant in the y direction, because of the inhomogeneity of the $\hat{\mathbf{I}}$ texture. A proper treatment would require the solution of a two-dimensional Schrödinger equation instead of Eq. (2). The variation of a is on the order of 50% and probably leads to some changes in our numerical results.

The fact that the first Bragg peak can be observed in the NMR spectrum attests to the presence of a well-correlated one-dimensional periodic structure. This is a fundamental property of the vortex-sheet state and a strong argument for its existence. The observation of one-dimensional periodicity suggests that collective hydrodynamic modes, such as the analog of a Tkachenko shear wave of an ordered vortex line lattice, with displacements perpendicular to the Ω axis, might be observable. One-dimensional periodicity exists also in smectic liquid crystals, in which a similar Goldstone mode, a coupled density oscillation, and the spacing b of the consecutive planes have been observed.⁷

This work was supported by the ROTA co-operation plan of the Finnish Academy of Sciences and the Russian Academy of Sciences. G.E.V. was supported in part by the Russian Fund for Fundamental Research, Grants No. 93-02-02687 and 94-02-03121, and Ü.P. received a scholarship from the Finnish Cultural Foundation.

¹Ü. Parts, E. V. Thuneberg, G. E. Volvek *et al.*, Phys. Rev. Lett. (in print).

²L. Landau and E. Lifshitz, Dokl. Akad. Nauk (USSR) **100**, 669 (1955).

³I. A. Fomin and V. G. Kamenskii, JETP Lett. **35**, 302 (1982).

⁴K. Maki and P. Kumar, Phys. Rev. B **16**, 182 (1977).

⁵For a review see M. M. Salomaa and G. E. Volovik, Rev. Mod. Phys. **59**, 533 (1987) or A. L. Fetter, in Prog. Low Temp. Phys., ed. D. F. Brewer (Elsevier Publ., 1986), Vol. X, p. 1.

⁶A. L. Fetter, J. A. Sauls, and D. L. Stein, Phys. Rev. B **28**, 5061 (1983).

⁷S. Chandrasekhar, *Liquid Crystals* (Cambridge University Press, Cambridge, 1977).

Published in English in the original Russian journal. Reproduced here with stylistic changes by the Translations Editor.